Complete open loop control of hysteretic, creeped and oscillating piezoelectric cantilevers

Micky Rakotondrabe, *member, IEEE*, Cédric Clévy and Philippe Lutz, *member, IEEE*

***Abstract*— The feedforward compensation of nonlinearities, i.e. hysteresis and creep, and unwanted vibrations in micromanipulators is presented in this paper. The aim is to improve the general performances of piezocantilevers dedicated to micromanipulation/microassembly tasks. While hysteresis is attenuated using the Prandtl-Ishlinskii inverse model, a new method is proposed to decrease the creep phenomenon. As no model inversion is used, the proposed method is simple and easy to implement. Finally, we employ an input shaping technique to reduce the vibration of the piezocantilevers. The experimental results show the efficiency of the feedforward techniques and their convenience to the micromanipulation/microassembly requirements.**

***Note to Practitioners*—The works presented in this article are motivated by the high performances required in micromanipulation and microassembly tasks. Such a domain requires high accuracy, sometimes submicrometric, and stability of the micromanipulators. While piezoelectric cantilever structures are very widespread in this domain, their nonlinearities and vibrations undeniably limit their performances such as accuracy and overshoots. This may be detrimental for the micromanipulation/microassembly tasks. Feedback control techniques could easily improve their performances but the sizes of accurate and large bandwidth sensors do not make them easily embarkable for micromanipulation/microassembly systems. Thus, controllers without sensors are of great interest. In this paper, we show that open loop control techniques (also called feedforward techniques) can improve the general performance of piezocantilevers dedicated to micromanipulation/microassembly tasks. We notice that the techniques can also be applied to other nonlinear and oscillating systems.**

***Index Terms*— Piezoelectric cantilever, microassembly/micromanipulation, hysteresis compensation, creep compensation, vibration compensation, input shaping.**

I. Introduction

Nowadays, miniaturized systems which integrate more intelligence and functionalities are required more and more. These systems are either micromechanisms (micro ball bearings, microgears, micromotors), micro-optical systems (switches, lasers) or hybrid Micro-Opto-Electro-Mechanical-Systems (MOEMS) like micro-scanners, microspectrometers, or micro-coils [1] [2] [3] [4] [5]. To produce them, monolithic microfabrication can be used but new perspectives are opened with micromanipulation/microassembly techniques, such as hybrid microassembly [6] [7].

One of the main characteristics of micromanipulation/microassembly systems is the high accuracy that they must have to perform tasks. According to the sizes of the manipulated microparts, the required accuracy may be submicrometric. For instance, fixing a micro lens at the tip of an optical fiber with 1μm of relative positioning error or 0.4μrad of orientation error may cause a loss of 50 % of the light flux [8]. In order to reach the required accuracy, microrobots, micromanipulators and gripping tools are designed differently from classical robots and manipulators. Depending on the nature of the micromanipulation/microassembly tasks, and notably on the shape of the manipulated microparts, several gripping tools can be used: microgrippers, needles, vacuum grippers, ice grippers, etc. For flexibility and accuracy reasons, microgrippers are very efficient [7]. Most of positioning and gripping systems are often based on active materials in order to avoid mechanical clearances and then to increase the accuracy. Among active materials, piezoelelectric ones are widespread and their use continues to grow due to their fast response time, high resolution and sensor capabilities. Piezoelectric materials are notably appreciated and very common in piezotube scanners for AFM microscopes, in piezocantilevers and microgrippers for micromanipulation/microassembly and in actuators for step-by-step microrobots. In the case of micromanipulation/microassembly, piezocantilevers and piezoelectric microgrippers (composed of two piezocantilevers) especially offer the possibility to estimate and to control the force at the same time as the positioning control [9] [10].

Unfortunately, like other active materials, performances of piezocantilevers (and piezoelectric materials in general) are strongly affected by nonlinearities. These nonlinearities, which are the hysteresis and the creep, appear in the voltage-strain transfer [11]. While piezoelectric materials present nonlinearities with large electric fields, bending structures (cantilevers) suffer from poorly damped vibrations.

Hysteresis and the creep indeniably influence on the positioning repeatability and the accuracy of the micromanipulation/microassembly systems. It also decreases the accuracy of the force estimation if such a technique is used in the systems. In addition, the vibration critically influences overshoot of micromanipulation forces and may cause damages of manipulated fragile microparts (biological parts, optical parts, etc.) or conversely a rigid micropart may cause the damage of a micromanipulator. Finally, controlling the force may make a release task successful in the presence of adhesion forces.

FEMTO-ST Institute, UMR CNRS 6174 - UFC / ENSMM / UTBM
Automatic Control and Micro-Mechatronic Systems depart., AS2M
24, rue Alain Savary
25000 Besançon - France
{mrakoton,cclevy,plutz}@femto-st.fr
Paper type: regular paper. First submission: June 2008.

Closed loop control techniques seem to be the best way to reach overall substantial performances (accuracy, repeatability, disturbances and vibration rejection, etc.). They also enable a robust control that takes into account the uncertainties or variations of models parameters [12] [13]. However, the use of closed loop control techniques in micromanipulation/microassembly is strongly limited by the difficulty to integrate sensors: sensors which are precise and fast enough are bulky (interferometers, triangulation optical sensors, camera-microscopes measurement systems, etc.) or difficult to fabricate [14]. As example, Fig. 1 depicts a microassembly system composed of a table for feeding the micro-objects, a microgripper to manipulate them and a camera-microscope measurement system for visual servoing or for human operator feedback. Additional light sources are often required to condition the visual measurement system best. This picture clearly shows how convenient measurement systems for micromanipulation/microassembly require a lot of space. Hence, an open-loop control technique is an alternative way to overcome this problem. Several studies demonstrated that open loop control techniques can be an attractive approach in micro/nano-applications: the overall performances have procured satisfactions [15] [16].

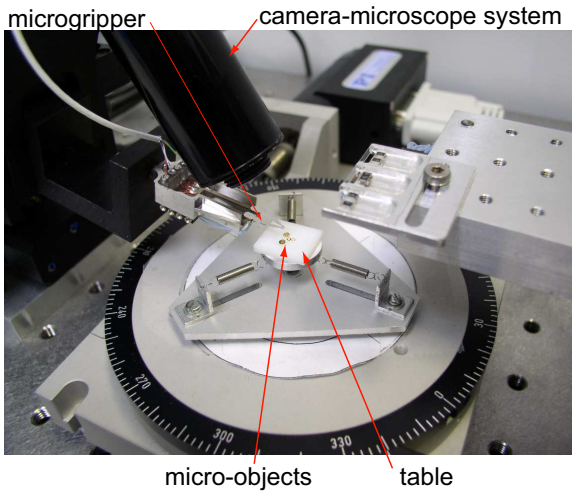

Fig. 1. Picture of a microassembly system composed of a piezogripper for manipulation, a table for feeding micro-objects and a camera-microscope measurement system.

In open loop control techniques, the hysteresis can be compensated by the use of feedforward inverse model. Several direct and inverse models have been used. Among them: the Preisach [17], the Prandtl-Ishlinskii [18] [19] and the Bouc-Wen models [9]. The Prandtl-Ishlinski is interesting for simplicity of its implementation, ease of obtaining its inverse analytical formulation and its accuracy.

Concerning the creep, different models have been used. In [19] [20], a logarithmic function is used. To compensate the creep, an opposite logarithmic model is established for the applied voltage so that the final piezoelectric strain will remain constant. Another approach is to model the creep by a linear dynamic operator [21]. In these two works, the linear dynamic operator is composed of many elementary first order operators. From an automatic point of view, the use of a linear dynamic model is very interesting because of ease of identification and control. To eliminate the creep, an inversion of the creep model is computed and used as a feedforward controller. However, this approach requires that the creep model is a bi-causal system, i.e. the direct model and its inverse should be causal.

Finally, to eliminate unwanted vibrations in piezoelectric materials, [21] [22] use once again linear dynamic models and their inversion. The interest is the ease of modeling and identification of the vibrations but the approach always requires bi-causal models and their invertibility. Furthermore, while the input shaping techniques have shown their efficiency with thermal microsystems [14], it may be of great interest for oscillating piezocantilevers.

Improving performances of piezoelectric materials, notably piezotube scanners, by eliminating the hysteresis and/or creep has been proved ([16] gives a survey). Works which accounts the vibrations in addition with these nonlinearities are yet uncommon [21] [22]. It is due to the fact that vibrations only appear with some geometrical structures and with a limited bandwidth of the acquisition system.

The core of this paper is the improvement of the performances of hysteretic, creeped and oscillating piezocantilevers dedicated to micromanipulation/microassembly tasks. The hysteresis is removed using the Prandtl-Ishlinskii inverse model because of its good accuracy and ease of implementation. For the creep, we always use a dynamic linear model but instead of inverting it, we propose a new method that does not require the bi-causality condition of the model. Concerning the vibrations, we propose the use of the ZV (Zero Vibration) input shaping technique. The experiments will show that the input shaping technique removes the unwanted vibrations without using the inversion model as well. It is important to note that while the thermal drift may be important in AFM applications [23], this is negligible in the application presented in this paper when the temperature variation is low [24].

First, an insight of the different compensation steps is presented. Then, the hysteresis compensation is detailed. After that, the analysis of the creep is presented and a new compensation approach is proposed. Finally, the method used to eliminate the vibrations ends the paper.

II. Principle of control

Fig. 2 presents a piezocantilever subjected to an electric excitation. U refers to the applied voltage and δ represents the resulting deflection.

There are different kinds of piezocantilever (unimorph, bimorph, etc.). If mathematical models are used instead of physical ones, their analysis and control synthesis are similar. From a control point of view, mathematical models are of great interest because of their independency from the physical characteristics of the system. In this paper, we use such models and the experiments are performed with a unimorph piezocantilever made up of a PZT-layer and a Copper layer. The sizes are: $300\mu m$ of total thickness ($200\mu m$ for the

piezolayer), $2mm$ of width and $15mm$ of active length. The whole experimental setup is composed of (Fig. 3-a and b):

- computer-dSPACE material for the controllers. The Matlab-Simulink ™ software is used for their implementation,
- a voltage amplifier,
- the previously described unimorph piezocantilever,
- and a laser sensor in order to identify the piezocantilever and to validate the resulting performances. The sensor has a $0.1\mu m$ of resolution and a high passband which enable the capture of the piezocantilever performances.

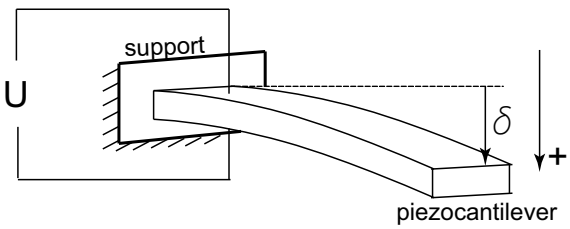

Fig. 2. A piezocantilever bends when subjected to an electrical excitation.

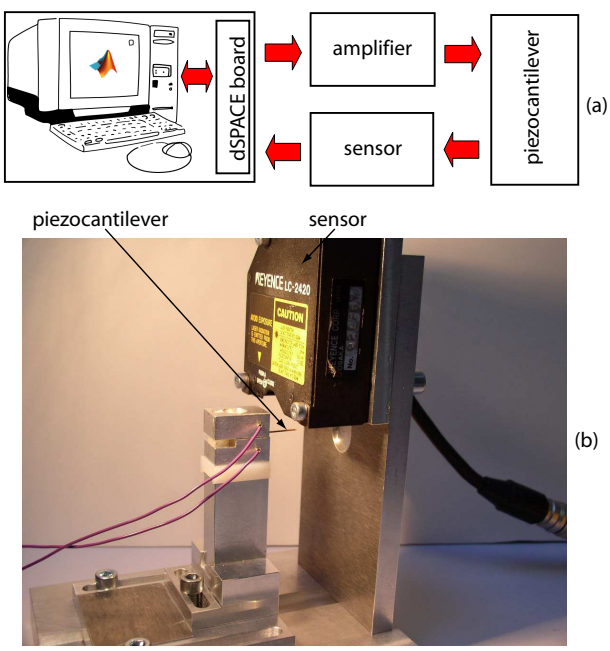

Fig. 3. The experimental setup: the piezocantilever is controlled through a computer-dSPACE material and an amplifier. A laser sensor is used to measure the piezocantilever deflection.

When a step input voltage is applied, the deflection reaches a final value after a transient part which is oscillating. If the constant input is still kept, a slow drift appears. This is the creep (Fig. 4-a). The settling time of the transient part is generally lower than $50ms$ and that of the creep is several minutes. The amplitude of the creep depends on the amplitude of the step input voltage. The hysteresis can be seen when plotting the deflection versus an applied sine input voltage (Fig. 4-b). The hysteresis in a piezocantilever is dynamic (rate-dependent) but it has been shown in previous works that this is equivalent to a static hysteresis (rate-independent) followed by a linear dynamic part [13]. Thus, the hysteresis only affects the static gain, i.e. the final value (before creep) of the step response.

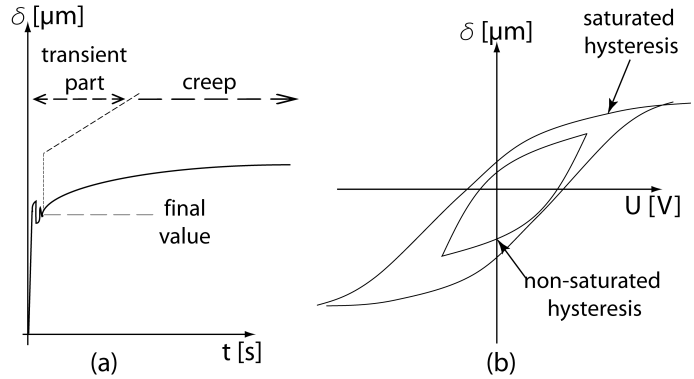

Fig. 4. The nonlinear behaviors of a piezocantilever: (a) the step response of a piezocantilever showing the transient part and the creep, (b) the hysteresis.

In feedforward control techniques, precise models are needed. When there are several objectives, for example the cancellation of the hysteresis, creep and vibrations at the same time, the model of each behaviour is needed. Sometimes, one model is sufficient to account for two behaviours [20]. In this paper, each behaviour is independently modelled for more precision. The modeling, identification and compensation are performed step by step. These are as follows:

- first, the hysteresis is analyzed and compensated. The Prandtl-Ishlinskii (PI) model is used,
- second, the creep of the new system, ie. of the piezocantilever with hysteresis compensation, is identified and compensated. A new and simple compensation method which does not require an inversion model is proposed,
- finally, the oscillation of the creep and hysteresis compensated system is modelled and attenuated using the Zero Vibration (ZV) input shaping technique.

III. Hysteresis compensation

The Prandtl-Ishlinskii (PI) static hysteresis model is used in this section. In fact, since it is based on the superposition of many elementary operators like the Preisach hysteresis model, it can provide a very high accuracy. In addition, the ease of implementation of the PI model causes it to be used for various systems.

A. The Prandtl-Ishlinskii (PI) static hysteresis model

Each element that composes a PI model is a backlash characterized by a threshold r_i and a weighting coefficient w_i (Fig. 5-a) [25]. The weighting coefficient is a gain that determines the slope of the backlash straights.
The identification of a hysteresis curve should be done with the maximal value of the input voltage U that will be used. This especially depends on the range of applications. After that, the corresponding hysteresis curve should be shifted so

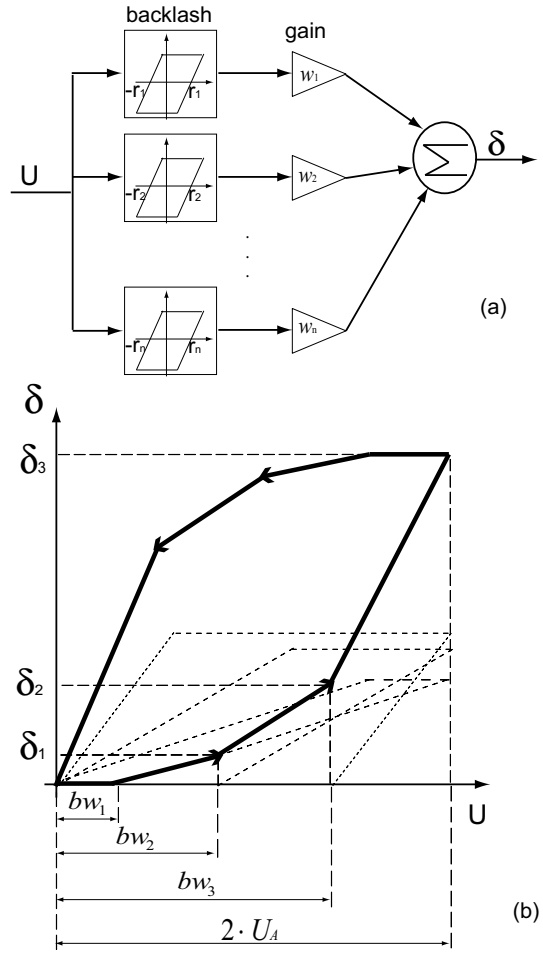

Fig. 5. Diagrams showing the principle of the PI static hysteresis model: (a) the PI hysteresis model is a sum of elementary backlash operators, (b) diagram showing an example of hysteresis obtained with three elementary operators [26].

that it is in the positive section of the input-output (U, δ) plane. Fig. 5-b shows an example of a hysteresis curve approximated by three elementary backlashes [26]. In Fig. 5, $bw_i = 2 \cdot r_i$ is the bandwidth and U_A is the amplitude of the sine input signal before shifting. From the figure, the kth output can be formulated as follows:

$$\delta_k = \sum_{i=1}^{k} (bw_{k+1} - bw_i) \cdot w_i \tag{1}$$

From the previous equation, a tensorial formulation can be obtained:

$$\{\delta\} = [A] \cdot \{w\} \tag{2}$$

where $[A]$ is a triangular matrix constructed from the different bandwidth values.

To model and identify a hysteresis by the PI model, the steps are as follows.

- Apply at least half a period of sine voltage U to the piezo-cantilever. The amplitude of the corresponding output δ should cover the end use range.
- If the obtained hysteresis curve is not in the positive section of the (U, δ)-plane, shift the curve,
- Define the number n of the elementary backlashes,
- Split the input U domain into $n + 1$ uniform or non-uniform partitions. For example, Fig. 5-b depicts four partitions and presents an approximation of hysteresis with three backlashes. The bandwidth bw_i and the output vector $\{\delta\}$ are easily obtained according to the Fig. 5-b,
- Construct the matrix $[A]$ from the bandwidth bw_i using the (equ 1) and (equ 2),
- Finally, compute the parameter $\{w\}$ using the following formula:

$$\{w\} = [A]^{-1} \cdot \{\delta\} \tag{3}$$

B. The PI inverse model

To compensate a hysteresis that has been modelled with a PI model, another PI hysteresis model is put in cascade with it (Fig. 6-a). In Fig. 6-a, δ_h represents the reference during the hysteresis compensation. The compensation principle is given in Fig. 6-b: to obtain a linear input-output (δ_h, δ) with a unit gain, the real system curve (U, δ) and the compensator curve (δ_h, U) should be symmetric [18].

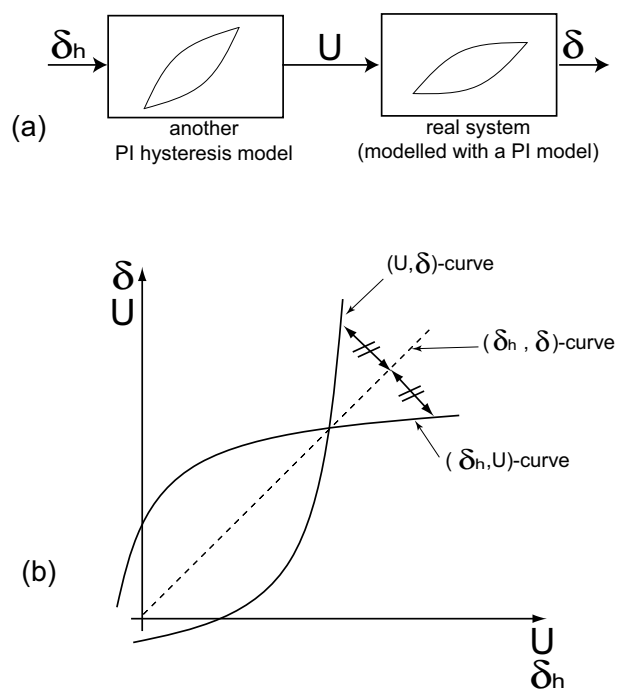

Fig. 6. Diagrams showing the compensation of a hysteresis: (a) the direct hysteresis can be compensated by another hysteresis put in cascade with it, (b) the direct hysteresis and its compensator should be symmetric relative to a linear curve [18].

Like the PI direct model, each elementary operator of the PI inverse model is characterized by a bandwidth bw'_i, a threshold $r'_i = \frac{bw'_i}{2}$ and a weighting gain w'_i. From the principle of Fig. 6-b, they are computed as follows [18]:

$$r'_k = \sum_{j=1}^{k} w_j \cdot (r_k - r_j) \quad ; \quad k = 1 \cdots n \tag{4}$$

and

$$w'_1 = \frac{1}{w_1}$$

$$w'_k = \frac{-w_k}{\left(w_1 + \sum_{j=2}^{k} w_j\right) \cdot \left(w_1 + \sum_{j=2}^{k-1} w_j\right)} \quad ; \quad k = 2 \cdots n \tag{5}$$

C. Experiments

Following the identification steps described below, a sine voltage with $40V$ of amplitude is applied to the piezocantilever. It corresponds to a deflection of $20\mu m$. The frequency is chosen so that neither the dynamic part nor the creep of the piezocantilever influences the curve. In our case, the cutting frequency of the dynamic part (ω^c_{dyn}) is nearly $3000rad/s$ while the one of the creep (ω^c_{creep}) is less than $0.05rad/s$ for unimorph piezocantilevers. If the identification frequency is higher than ω^c_{dyn}, the phase of the dynamic part will distort and revolve the hysteresis curve. If it is lower than ω^c_{creep}, additional deflection due to the creep will also distort the hysteresis curve. In this experiment, we use a frequency of $0.628rad/s$ ($0.1Hz$). Fig. 7 shows the experimental result and the simulation of the identified PI model when two input voltage amplitudes are used (resp. $U = 20V$ and $U = 40V$).

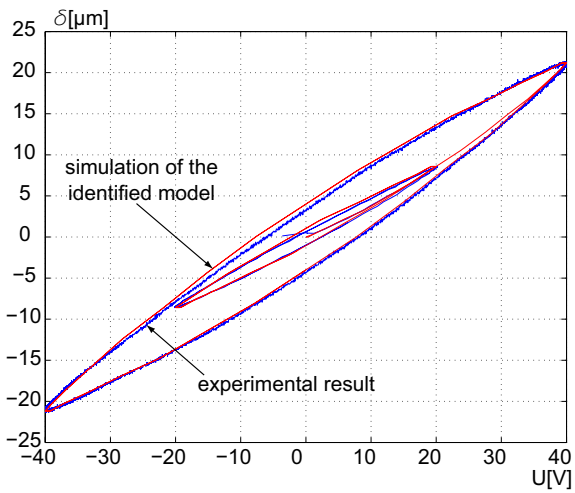

Fig. 7. Curves displaying the hysteresis of the piezocantilever (with $f = 0.1Hz$): experimental results and simulation of the identified PI model with amplitudes $U = 20V$ (inner loop) and $U = 40V$ (outer loop).

The computed PI inverse model has been implemented. Fig. 8 gives the experimental results and points out that the hysteresis has been reduced into 2.5% ($= \frac{h}{H} \cdot 100\%$) instead of nearly 20% without compensation.

IV. Creep compensation

In this section, we analyze and control the creep of the linearized system, i.e. system with the hysteresis compensator. The new input is δ_h and the output is still δ. To open loop control the creep, it is necessary to identify and model it. For that, a step input with $\delta_h = 20\mu m$ is applied. Despite the final

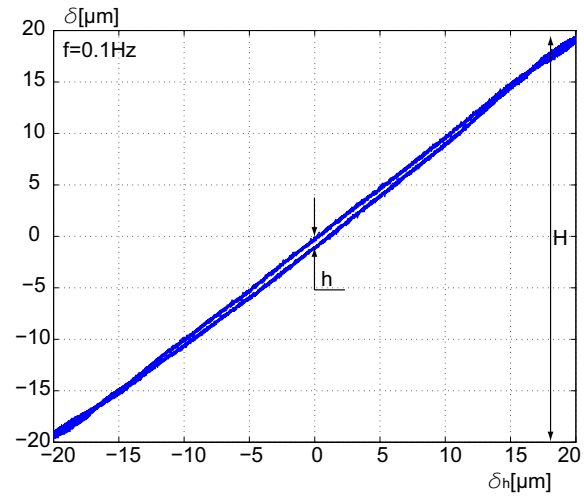

Fig. 8. An experimental result displaying the measured deflection vs. the reference input when using the hysteresis compensation.

value δ_{fv} which is equal to the input reference, a creep greater than 40% ($= \frac{creep}{\delta_{fv}} \cdot 100\%$) appears along $600s$ of the period (Fig. 9). To attenuate this creep, an approach that does not need model inversion is proposed in this section.

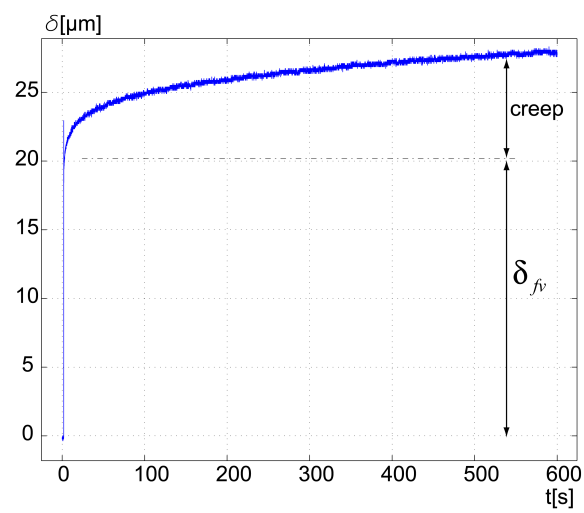

Fig. 9. An experimental result displaying the measured deflection when a step input reference is applied. The result was obtained with the piezocantilever with hysteresis compensation.

A. Compensation principle

Regarding Fig. 9, the deflection δ can be defined as the sum of two signals: the constant value δ_{fv} and the additional drift $creep(t)$. Let $K = \frac{\delta_{fv}}{\delta_h}$ be the linear static gain and $creep(s) = C(s) \cdot \delta_h(s)$ be the creep model. Without considering the transient part, we have (Fig. 10-a):

$$\frac{\delta}{\delta_h} = (K + C(s)) \tag{6}$$

The static gain K may differ from 1 according to the linearization accuracy during the previous section. To compensate the

creep $C(s)$, we propose the principle shown in Fig. 10-b. In the proposed method, the real parameter $\frac{1}{K}$ is used to compensate the static gain K if the latter differs from 1.

From Fig. 10-b, the equation of the creep compensator is easily derived:

$$\frac{\delta_h}{\delta_c} = \frac{1}{(K + C(s))} \tag{7}$$

where δ_c is the new reference input.

We remark that there is no bi-causality condition imposed on the model $C(s)$. Indeed, if $Num(s)$ and $Den(s)$ are respectively the numerator and the denominator of $C(s)$, we have:

$$\frac{\delta_h}{\delta_c} = \frac{Den(s)}{(K \cdot Den(s) + Num(s))} \tag{8}$$

As $\deg(Den(s)) \geq \deg(Num(s))$ (causality of natural systems), where $\deg(.)$ is the degree of a polynomial, the compensator is always causal.

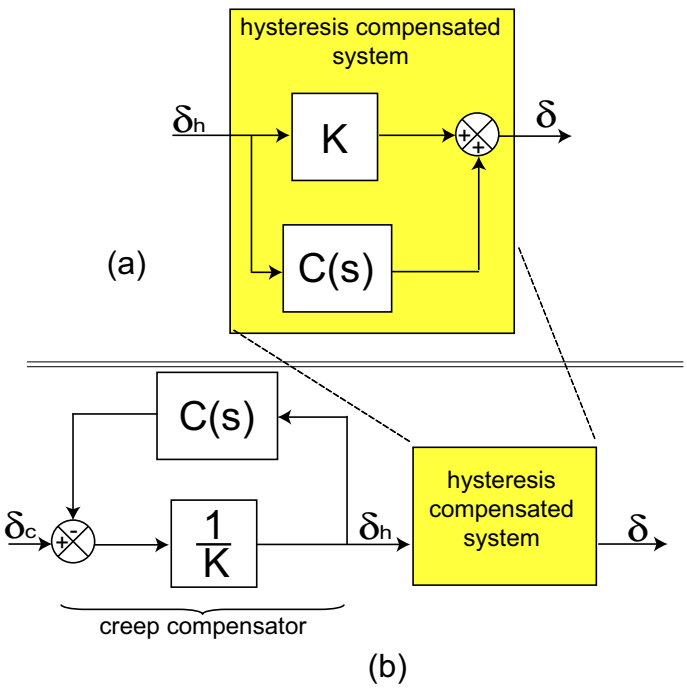

Fig. 10. (a) Bloc-diagram displaying the new system: the piezocantilever with the hysteresis compensator. (b) Bloc-diagram of the new system (piezocantilever + hysteresis compensator) and of the creep compensator.

Using (equ 6) and (equ 7), we derive the transfer function of the new compensated system:

$$\frac{\delta}{\delta_c} = (K + C(s)) \cdot \frac{1}{(K + C(s))} = 1 \tag{9}$$

B. Experiments

To identify $C(s)$, the creep part is separated from the step response curve ie. the drift part of the curve in Fig. 9 is separated and identified. Then, we have the curve pictured in Fig. 11. The identification of $C(s)$ is performed as follows: 1) an order model is chosen, 2) an ARMAX (Auto Regressive Moving Average with eXternal inputs) model and the matlab software are used to determine the parameters [27], 3) the curve corresponding to the simulation and the experimental result are compared, 4) if they do not fit well, the order model needs to be increased and the identification process started again. The sampling time is $50ms$. For the experimented piezocantilever, a third model order is a good compromise between low-order (ie. low complexity) and good adequacy of the simulation/experimental curves (Fig. 11). The identified model is:

$$C(s) = 0.465 \cdot \frac{(16 \cdot s + 1) \cdot (203 \cdot s + 1)}{(3 \cdot s + 1) \cdot (34 \cdot s + 1) \cdot (444 \cdot s + 1)} \tag{10}$$

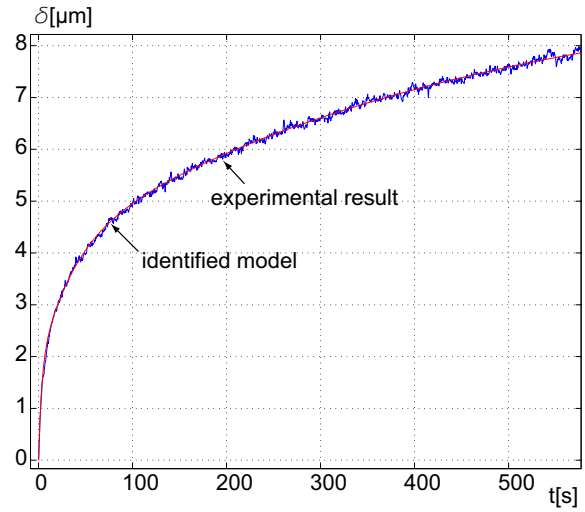

Fig. 11. Experimental curve (measured deflection) and simulation of the identified model of the creep phenomenon. The experimental curve corresponds to the drift pictured in Fig. 9.

The creep compensator is implemented and added to the previously implemented hysteresis compensator. The parameter $\frac{1}{K}$ has intentionally been left equal to 1 because the linear gain $K \approx 1$ according to Fig. 9. The result with a step input $\delta_c = 20\mu m$ is presented in Fig. 12. The zoom (Fig. 12-b) shows that the creep is reduced into less than 2.5%. However, there is a high overshoot in the transient part of the step response. This behaviour will be analyzed and compensated in the next section.

Fig. 13 pictures the experimental step response when the amplitude of the input reference step is $10\mu m$. It clearly shows that the performance still remains when the amplitude of the input is changed.

V. Dynamic compensation

Once again, a new system is obtained. It contains the piezocantilever, the hysteresis and the creep compensators. These are considered as low frequency characteristics because the hysteresis acts in the static gain while the creep has a high settling time. In this section, we are interested by the fast dynamic characteristics. It concerns the transient part of the

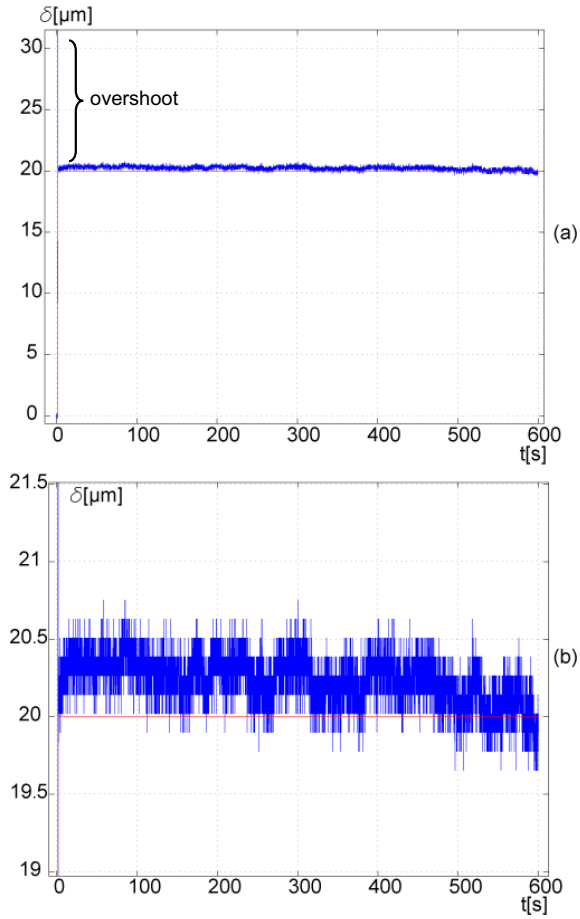

Fig. 12. Curves displaying the experimental results when using the proposed creep compensator, ie. creep compensator + hysteresis compensator + piezocantilever, the input reference being a step of $20\mu m$ of amplitude. (a) Measured deflection along $600s$ of duration. (b) Zoom of the measured deflection.

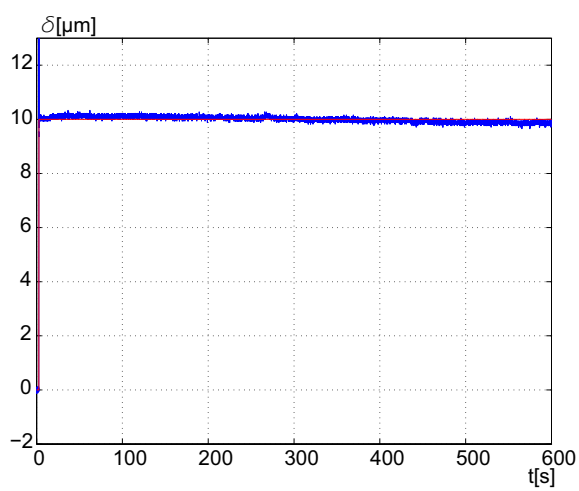

Fig. 13. Curve displaying the measured deflection when the input reference is a step with $10\mu m$ of amplitude.

new system. Indeed, in Fig. 9, before the output δ reaches the final value of $20\mu m$, it overshoots 62.5%. Such displacement overshoot causes high manipulation forces overshoot during micromanipulation/microassembly tasks and may be fatal for the manipulated microparts as well for the micromanipulators. In addition, the transient part is badly damped oscillating. In this section, the vibration and the overshoot are compensated. For that, the Zero Vibration (ZV) input shaping technique is used.

A. The ZV input shaping technique

There are different kinds of input shaping methods but the one presented here is the Zero Vibration (ZV) one. A panorama of other existing methods is given in [28]. The ZV input shaping method [29] is a simple technique to minimize the vibration in lightly damped systems. It is based on the convolution of a sequence of impulses called shaper and an input signal.

When an impulse is applied to an oscillating system, a vibration appears. Let ω_n be the natural frequency and ξ the damping ratio. When a second impulse is applied at time $T_d = T/2$, with $T = \frac{2\cdot\pi}{\omega_n\cdot\sqrt{1-\xi^2}}$, the vibration caused by the second impulse can cancel the one caused by the first impulse (Fig. 14-a) if the amplitudes of both are judiciously chosen. Hence, to apply any reference input δ_r, the previous sequence of impulses, also called shaper, is convolved with δ_r. Fig. 14-b shows the bloc-diagram of the shaper convolved with the input reference. As a result, for a step reference input, the control signal is a staircase with two steps.

If the identified parameters ω_n or ξ are quite different from the real parameters, a residual vibration will remain after compensation. Indeed, the vibration caused by the first impulse will not be cancelled by that of the second one because the phase between both and the amplitudes are not convenient. Therefore, if the overshoots of the two vibrations are very high, the resulting interfered signal may also have a high overshoot. To avoid such a problem, references [30] [31] propose robust Input Shaping techniques. These techniques can also be applied when the parameters vary according to the environmental disturbances. An alternative to robust Input Shaping techniques is to use more than two impulses in the shaper of the classic Zero Vibration technique. In this case, each impulse amplitude and the corresponding vibration are small. So, the resulting interfered signal will have a lower overshoot if any [32].

The computation of the shaper is described below. Let K be the static gain of the badly damped oscillating system. Its model is:

$$\frac{\delta}{\delta_c} = \frac{K}{\left(\frac{1}{\omega_n}\right)^2 \cdot s^2 + \frac{2\cdot\xi}{\omega_n}\cdot s + 1} \tag{11}$$

Consider A_i and t_i the amplitudes of the impulses and their application times (delays). Each vibration caused by each impulse has the following time-domain equation:

$$\delta_i(t) = KA_i \frac{\omega_n}{\sqrt{1-\xi^2}} e^{-[(t-t_i)\xi\omega_n]} \sin\left(\omega_n\sqrt{1-\xi^2}\,(t-t_i)\right) \tag{12}$$

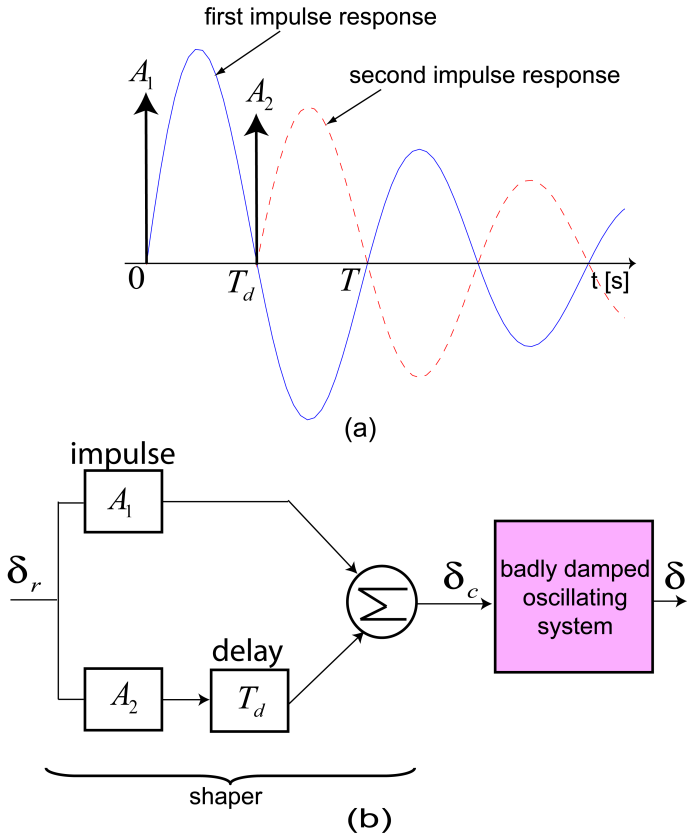

Fig. 14. Principle of the ZV input shaping techniques. (a) Two impulses can cancel the vibrations of a badly damped oscillating system if their amplitudes and application times are convenient. (b) For any input reference δ_r, the vibration can be compensated by convolving it with the shaper (composed of the delayed impulses).

To obtain an output without any vibration, the following equation is used:

$$\sum_{i=1}^{m} \delta_i(t) = 0 \tag{13}$$

where m is the number of impulses in the shaper.

In the ZV input shaping technique, the two following conditions must also be completed:

$$\begin{cases} \sum_{i=1}^{m} A_i = 1 \\ A_i > 0 \end{cases} \tag{14}$$

Consider $\beta = e^{-\frac{\xi.\pi}{\sqrt{1-\xi^2}}}$. The solutions are:

$$A_i : \begin{pmatrix} A_1 = \frac{a_1}{(1+\beta)^{m-1}} \\ A_2 = \frac{a_2}{(1+\beta)^{m-1}} \\ \vdots \\ A_m = \frac{a_m}{(1+\beta)^{m-1}} \end{pmatrix} \tag{15}$$

$$t_i : \begin{pmatrix} t_1 = 0 \\ t_2 = T_d \\ \vdots \\ t_m = (m-1) \cdot T_d \end{pmatrix}$$

where m is the number of impulses in the shaper, a_i indicates the ith monomial of the polynomial from $(1+\beta)^{m-1}$. We have $a_1 = 1$ and $a_m = \beta^{m-1}$.

B. Experiments

The natural frequency and the damping ratio were identified. A step response was used for that. The experimental result of Fig. 15 clearly shows an oscillation characterized by 62.5% $(= \frac{\delta_{\max} - \delta_{fv}}{\delta_{fv}} \cdot 100\%)$ of overshoot and a settling time more than $65ms$. Using the ARMAX method and matlab software, the model of the (equ 11) was identified and plotted with the experimental result:

$$\frac{\delta}{\delta_c} = \frac{1}{4.5 \times 10^{-8} \cdot s^2 + 4.2 \times 10^{-6} \cdot s + 1} \tag{16}$$

with $\xi = 0.01$ and $\omega_n = 4713 rad/s$.

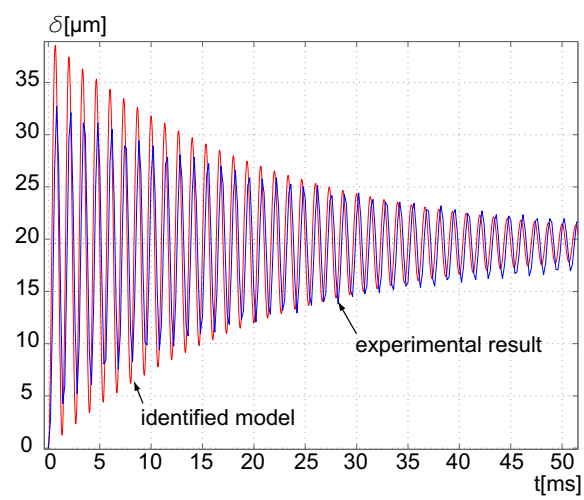

Fig. 15. Step response of the badly damped system (piezocantilever + hysteresis compensator + creep compensator): the experimental result (measured deflection) and the simulation result of the identified model.

The shaper has been computed and implemented in cascade with the two previous compensators (hysteresis and creep compensators). Fig. 16 presents the bloc-diagram. In order

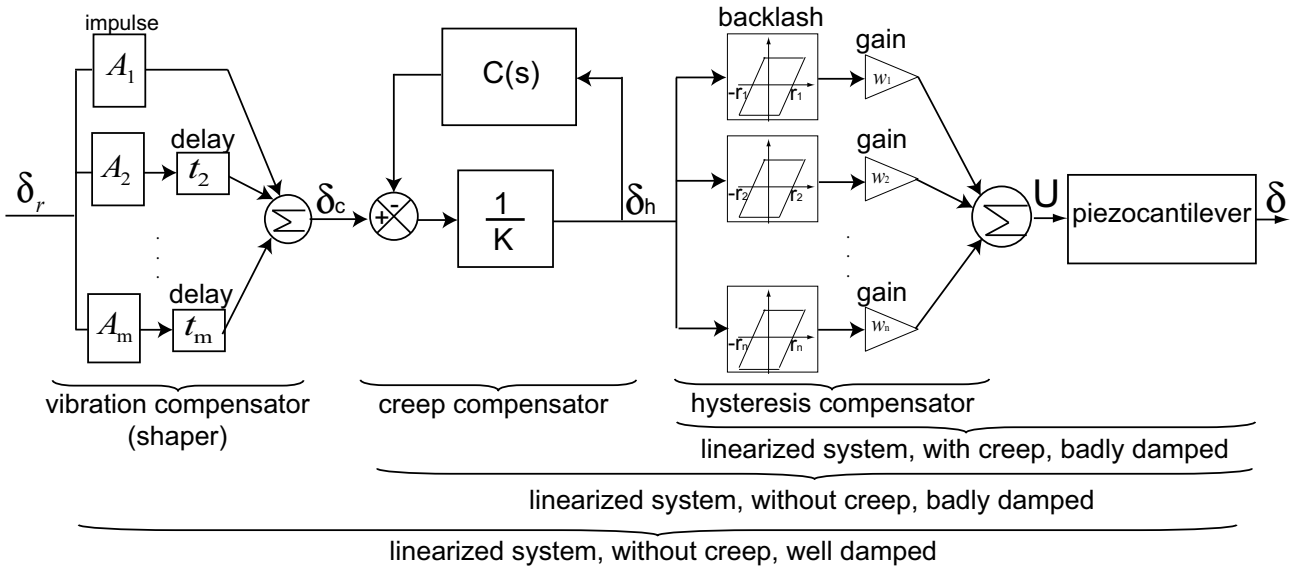

Fig. 16. Bloc-diagram of the complete compensation.

TABLE I

Performances of the piezocantilever with hysteresis, creep and vibration compensation.

	Overshoot	Settling time
Uncompensated vibration	62.5%	$82ms$
Compensated vibration (with 2 impulses shaper)	$negligible$	$24ms$
Compensated vibration (with 3 impulses shaper)	0%	$17ms$

to compare the results, a shaper with two impulses and a shaper with three impulses were computed and tested. The resulting piezocantilever's deflections were compared to the one when there is no shaper, ie. no vibration compensator. The aim is to clearly show the contribution of this vibration compensator. First, we have performed experiments with a step reference input having $\delta_r = 20\mu m$ of amplitude. The step responses indicate that the performances do not increase substantially when the impulse number is greater than three. Fig. 17 shows the experimental results of the compensated (shaper with 2 and 3 impulses) and of the non-compensated system. Table I summarizes the performances. They point out that the initial overshoot of 62.5% becomes negligible with a 2-impulse shaper and disappears with a 3-impulse shaper. In addition, a high reduction of the settling time is obtained.

Next, a harmonic experiment is performed in order to evaluate the performances more accurately. The results are given in Fig. 18. They show that the resonance peak of the uncompensated vibration is more than $20dB$. It is reduced into less than $2dB$ when using a two-impulse shaper and becomes completely removed with a three-impulse shaper. While the harmonic experiments confirm the step response experiment in general, the former gives an accurate comparison between the performances furnished by the two kinds of shapers.

Finally, Fig. 19-a depicts the linearity of the input-output obtained with a sine input reference ($f = 1Hz$) plane while and Fig. 19-b pictures the absence of drift when a step input

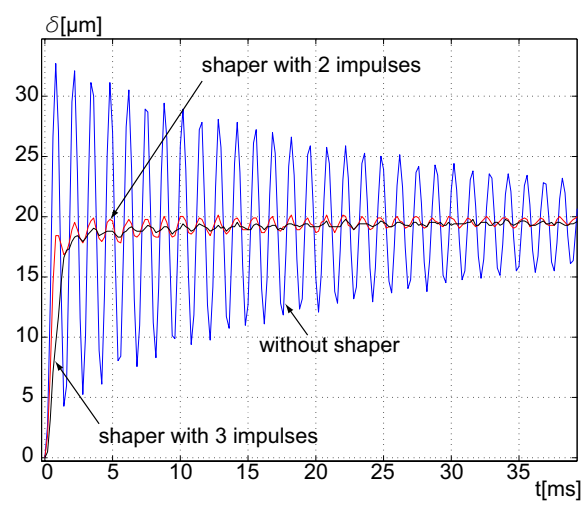

Fig. 17. Step response of the system with vibration compensation, ie. piezocantilever + hysteresis compensator + creep compensator + vibration compensator (shaper). The different curves are obtained with a 2-impulse shaper and a 3-impulse shaper. The curve obtained without shaper (ie. without vibration compensator as in Fig. 15) has been added in order to compare with those with shaper.

reference ($\delta_r = 20\mu m$) is applied. These results clearly show that the three compensators are compatible. Indeed, individual performances provided by each compensator are maintained when combining them. Such a case is respected if the identification of the behavior and computation of the controllers are respected:

- the hysteresis is identified at a frequency that is neither too low or too high. The creep phenomenon and the dynamic part do not influence the hysteresis curve in this case,
- the creep is identified in the static mode. A step response would provide better accuracy,
- the dynamic part is identified by using the transient part of the step response. A harmonic analysis can also be used if the system has been linearized.

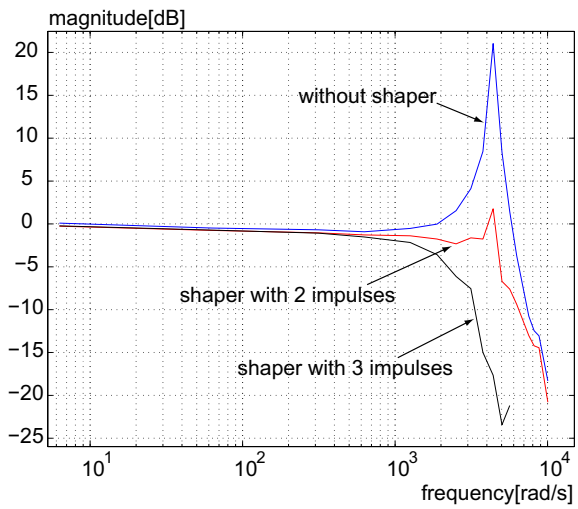

Fig. 18. Harmonic response of the system with vibration compensation, ie. piezocantilever + hysteresis compensator + creep compensator + vibration compensator (shaper). The different curves are obtained with a 2-impulse shaper and a 3-impulse shaper. The curve obtained without shaper (ie. without vibration compensator) has been added in order to compare with those with shaper.

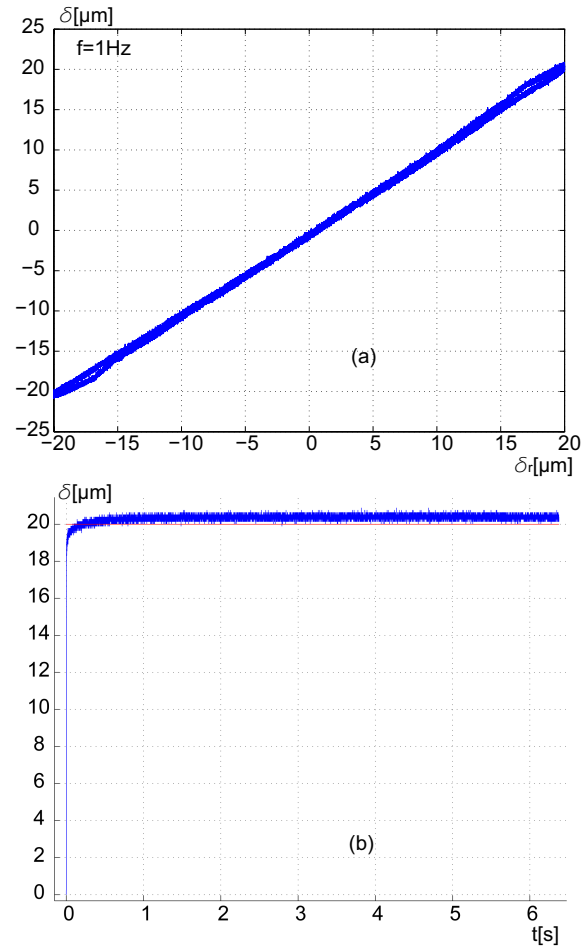

Fig. 19. Curves displaying the linearity and the absence of the creep of the final system, ie. piezocantilever + hysteresis compensator + creep compensator + shaper.

VI. Conclusion

This paper presents the compensation of the hysteresis, creep and vibration in piezocantilevers used for precise micromanipulation/microassembly. The necessity to use open-loop control, and then without sensors, raises the fact that available convenient sensors are bulky. So the aim of the paper presents the feedforward compensation of these three phenomena by identifying and compensating them step-by-step and successively. The paper especially applies the presented open-loop control techniques to piezocantilevers that are used for micromanipulation and microassembly.

The hysteresis nonlinearity was first reduced. Because of its accuracy and ease of implementation, the Prandtl-Ishlinskii (PI) inverse model was used. It has permitted the reduction of the hysteresis from 20% to less than 2.5%. After reducing the hysteresis, the creep is compensated. The creep compensator is implemented in cascade with the piezocantilever and the previous hysteresis compensator. A new method was proposed to compensate the creep. Its major advantage is that no inverting model is required. Hence, it does not require any condition on the bi-causality of the creep model. The experimental results show the reduction of the creep from 40% into less than 2.5%. Finally, the vibration of the badly damped system, ie. the hysteresis and creep compensated system, is analyzed and controlled. The chosen compensation method is the Zero-Vibration (ZV) input shaping. While the overshoot initially 62.5% is completely removed, the settling time is reduced by more than three times.

The works reported in this paper have confirmed that feedforward controllers can give general performances such as accuracy, zero-overshoot and speed required for a particular set of applications in the domain of micromanipulation/microassembly. Such controllers are of great interest because the costs, sizes and performances of existing sensors limit their use in this domain. The results presented in this paper are not only well adapted for positioning in micromanipulation/microassembly tasks but also for force estimation in them. Indeed, future work will be focused on the estimation of the manipulation force applied by a piezocantilever taking into account the linearization and vibration compensation described in this paper. Finally, robustness of the open-loop controllers relative to parameter variations, due to the environment for instance, will also be analyzed in our future works.

ACKNOWLEDGMENT

This work is supported by the French research project NANOROL (ANR N^oPSIROB07_184846).

REFERENCES

[1] N. Dechev, W. L. Cleghorn and J. K. Mills, "Microassembly of 3-D MEMS structures utilizing a MEMS microgripper with a robotic manipulator", IEEE ICRA (International Conference on Robotics and Automation), pp.3193-3199, Taipei, Taiwan, 2003.

[2] T. Udeshi and K. Tsui, "Assembly sequence planning for automated micro assembly", IEEE ISATP (International Symposium on Assembly and Task Planning), 2005.

[3] D. O. Popa, "High yield automated MEMS assembly: compliant snap-fastener design, precision robotics, and assembly evaluation", IEEE IROS (International Conference on Intelligent Robots and Systems), San Diego CA USA, 2007.

[4] N. Dechev and M. Basha, "Robotic microassembly of 3D MEMS structures", IEEE Transactions on Automation Science and Engineering, Vol.3, pp.207-215, 2008.

[5] W. Lin and W. J. Chen, "Fiber assembly of MEMS optical switches with U-groove channels", IEEE Transactions on Automation Science and Engineering, pp.207-215, 2008.

[6] A. N. Das, J. Sin, D. O. Popa and H. E. Stephanou, "On the Precision Alignment and Hybrid Assembly Aspects in Manufacturing of a Microspectrometer", 4th IEEE Conference on Automation Science and Engineering, 2008.

[7] C. Clévy, A. Hubert and N. Chaillet, "Flexible Micro-Assembly System Equiped with an Automated Tool Changer", Journal of micro-nano mechatronics, Vol.4, Issue.1,pp.59-72, 2008

[8] C. Gartner, V. Blumel, A. Kraplin and T. Possner, "Micro-assembly processes for beam transformation systems of high-power laser diode bars" MST news I, pp.23-24, 2000.

[9] M. Rakotondrabe, Y. Haddab and P. Lutz, "Nonlinear modeling and estimation of force in a piezoelectric cantilever", IEEE/ASME AIM (Internationl Conference on Advanced Mechatronics), Zurich Switzerland, 2007.

[10] M. Rakotondrabe, C. Clévy and P. Lutz, "modeling and robust position/force control of a piezoelectric microgripper", IEEE CASE (International Conference on Automation and Engineering), pp.39-44, Scottsdale AZ USA, 2007.

[11] J. L. Pons, "Emerging actuator technology: a micromechatronic approach", Wiley, ISBN: 0-470-09197-5, 2005.

[12] K. K. Leang and S. Devasia, "Hysteresis, creep, and vibration compensation", IFAC Conference on Mechatronic Systems, pp.283-289, 2002.

[13] M. Rakotondrabe, Y. Haddab and P. Lutz, "Quadrilateral modeling and robust control of a nonlinear piezoelectric cantilever", IEEE Transactions on Control Systems Technology, Vol.17, Issue 3, pp.528-539, May 2009.

[14] D. O. Popa and B. H. Kang and J. T. Wen and H. E. Stephanou and G. Skidmore and A. Geisberger, "Dynamic Modeling and Input Shaping of Thermal Bimorph MEMS Actuators", IEEE ICRA (International Conference on Robotics and Automation), pp.1470-1475, 2003.

[15] B. Borovic and A. Q. Liu and D. Popa and H. Cai and F. L. Lewis, "Open-loop versus closed-loop control of MEMS devices: choices and issues", Journal of Micromechechanics and Microengineering, Vol.15, N^o10, pp.1917-1924, 2005.

[16] S. Devasia, E. E. Eleftheriou, R. Moheimani, "A survey of control issues in nanopositioning", IEEE Transactions on Control Systems Technology, Vol.15, N^o5, pp.802-823, 2007.

[17] A. Dubra and J. Massa and C.l Paterson, "Preisach classical and nonlinear modeling of hysteresis in piezoceramic deformable mirrors", Optics Express, Vol.13, N^o22, pp.9062-9070, 2005.

[18] K. Kuhnen and H. Janocha, "Inverse feedforwrad controller for complex hysteretic nonlinearities in smart-materials systems", Control of Intelligent System, Vol.29, N^o3, 2001.

[19] B. Mokaberi and A. A. G. Requicha, "Compensation of scanner creep and hysteresis for AFM nanomanipulation", IEEE Transactions on Automation Science and Engineering, Vol.5, N^o2, pp.197-208, 2008.

[20] H. Jung, J.Y. Shim and D. Gweon, "New open-loop actuating method of piezoelectric actuators for removing hysteresis and creep", Review of Scientific Instruments, 71 (9), pp.3436-3440, 2000.

[21] D. Croft, G. Shed and S. Devasia, "Creep, hysteresis and vibration compensation for piezoactuators: atomic force microscopy application", ASME Journal of Dynamic Systems, Measurement and Control, 2001.

[22] G. M. Clayton, S. Tien, S. Devasia, A. J. Fleming and S. O. R. Moheimani, "Inverse-feedforward of charge-controlled piezopositioners", Mechatronics, 18, pp.273-281, June 2008.

[23] B. Mokaberi and A. A. G. Requicha, "Drift compensation for automatic nanomanipulation with scanning probe microscopes", IEEE Transactions on Automation Science and Engineering, pp.199-207, 2006.

[24] M. Rakotondrabe, C. Clévy and P. Lutz, "H-inf deflection control of a unimorph piezoelectric cantilever under thermal disturbance", IEEE IROS (International Conference on Intelligent Robots and Systems), San Diego CA USA, 2007.

[25] M. A. Krasnosel'skii and A. V. Pokrovskii, "Systems with hysteresis", Springer-Verlag, Berlin, 1989.

[26] A. Falvo, F. Furgiuele and C. Maletta, "Two-way shape memory effect of a Ti rich NiTi alloy: experimental measurements and numerical simulations", IOP Smart Materials Structures, pp.771-778, 2007.

[27] L. Ljung, "System identification toolbox", The matlab user's guide.

[28] T. Singh and W. Singhose, "Tutorial on input shaping/time delay control of maneuvering flexible structures", American Control Conference, pp.1717-1731, 2002.

[29] N. C. Singer, W. P. Seering and K. A. Pasch, "Shaping command inputs to minimize unwanted dynamics", Patent N^oUS-4.916.635, 1990.

[30] N. C. Singer and W. P. Seering, "Preshaping command inputs to reduce system vibration", ASME Journal of Dynamic Systems, Measurement and Control, Vol.112, pp.76-82, march 1990.

[31] W. Singhose, S. Derezinski and N. Singer, "Extra-insensitive inputr shapers for controlling flexible spacecraft", AIAA Journal of Gruidance, Control and Dynamics Vol.19, N^o2, pp.385-391, 1996.

[32] M. Rakotondrabe, C. Clévy and P. Lutz, "Hysteresis and vibration compensation in a nonlinear unimorph piezocantilever", IEEE IROS (International Conference on Intelligent Robots and Systems), Nice France, 2008.

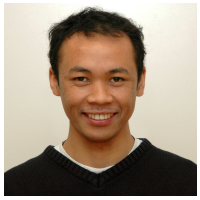

Micky Rakotondrabe (S'05, M'07) received the engineering diploma from the Institut Supérieur de Technologie du Nord (ISTN - ICAM), Lille, France, in 2002, the DEA diploma (M.Sc. equivalent) in automatic control from the Institut National des Sciences Appliquées (INSA), Lyon, France, in 2003, and the Ph.D. degree in automatic control from the Université de Franche-Comté, Besançon, France, in 2006.

Since September 2007, he has been an Associate Professor with the Université de Franche-Comté and a researcher with the FEMTO-st Institute. His field of research concerns the Control Theory applied to microsystems and microrobots. He has also contributed to the design, the development and control of microfactory during his PhD dissertation.

Cédric Clévy graduated from the Ecole Normale Supérieure de Cachan, France in 2001 received his master degree of Mechanical engineering, Automatics and Automation in 2002 and his Ph. D. degree of automatics in 2005. Since 2006, he has been an Associate Professor at the University of Franche-Comté, Besançon, France working at the FEMTO-ST laboratory. His research interests are design and control of micro-robotic, micro-factories, micro-assembly systems oriented to optical components.

Philippe Lutz (M'07) joined the University of Franche-Comté,Besançon as a Professor in 2002. He is currently the head of the research group "Automated Systems for Micromanipulation and Micro-assembly", AS2M department, FEMTO-ST. His research activities are focussed on the design and the control of micromechatronic systems. He teaches at the master level the design of Mechatronic Systems, Production System, and Control Theory.

He received the Engineer degree from the National School of Mechanics and Microtechnology (ENSMM), in 1990 and the Ph.D. in automation and computer science degree from the University of Franche-Comté, Besançon, France, in 1994. He was an Associate Professor with the INSA, Strasbourg, since 1994 until 2002. During this period, he has led the Mechatronics activities and developed research on inventive theory for solving problems.